

Original Article

Performance of Radial Basis Function and Group Method of Data Handling-Type Neural-Networks in Flammability Characteristics Prediction of PMMA

Mohammed Okoe Alhassan^{1*,4}, Stephen Eduku², Doreen Ama Amoah¹, Joseph Sekyi-Ansah¹, Felix Uba³

¹Department of Mechanical Engineering, Takoradi Technical University, Takoradi, Ghana.

²Department of Electrical & Electronic Engineering, Takoradi Technical University, Takoradi, Ghana

³Department of Mechanical and Manufacturing Engineering, University of Energy and Natural Resources, Sunyani, Ghana

⁴Department of Energy and Petroleum Engineering, University of Energy and Natural Resources, Sunyani, Ghana.

^{1*}Corresponding Author : mohammed.alhassan@ttu.edu.gh

Received: 02 March 2023

Revised: 19 April 2023

Accepted: 09 May 2023

Published: 25 May 2023

Abstract - In this paper, characterization of polymers fire behavior is studied for predicting the thermophysical flammability characteristics from developed supervised machine learning (SML) models. In the first stage, polymethyl methacrylate (PMMA) flammability properties, total heat release (THR) and heat release capacity (HRC) were examined and measured based on conducted micro-scale combustion calorimetry (MCC) experiments at varying heating rates (β) of milli-gram masses (m) ranging (0.1 - 3.5 Ks⁻¹) and (1 - 3.5 mg) respectively. Normalized experimental data was then used to develop SML models, radial basis function (RBF) and group method of data handling (GMDH-type) neural networks (NN) using m and β as input variables for performance prediction of HRC and THR. GMDHNN model performed remarkably well, attaining nominal errors in predicting HRC. Also, in estimating THR, RBFNN attained values with improved outcomes as compared to GMDHNN; hence, RBFNN performed relatively better in predicting THR. Overall, both ML algorithms performed well; nonetheless, GMDHNN outperformed RBFNN for prediction. Moreover, the GMDHNN and RBFNN models provided the lowest mean errors compared with HRC outcomes for PMMA from other HRC estimation models in the literature. As a result, both GMDHNN and RBFNN serve as applicable tools for PMMA flammability properties estimation based on the MCC fire test.

Keywords - Flammability, Group method of data handling-type neural-network, Microscale combustion calorimetry, Polymethyl Methacrylate (PMMA), Radial basis function neural-network.

1. Introduction

In light of the need for new heat- and fire-resistant materials in recent years, it is essential to be able to estimate the intrinsic flammability qualities of interest from suitable estimating methods before constructing these flame-resistant materials [1]. The important flammability properties of heat-releasing capacity (HRC) and the total heat released (THR) have been used to characterize and explain fire behaviors of materials, assisting in the development of polymers' flame-retardant properties [2].

For this purpose, experiments are conducted based on pyrolysis and combustion processes, representing the combustion properties at various fire scales, to study how combustible materials behave in a fire. To date, several fire calorimetry test methods, from macro to micro, have been established and developed to look at material flammability behaviors [3-5]. Small-scaled microscale combustion

calorimetry (MCC) [6] is the most frequently used "miniature" fire conducted experiment to evaluate and study the dynamic and static parameter behavior of material from the combustion process when subjected to fire in conformity to ASTM D7309-13 [7], "Method-A" standards.

To estimate this MCC flammability characteristics (THR and HRC), conventional methods have been used to conduct molecular structure model analysis based on material functional groups or molecular moiety properties established in Ref. [1, 7-13]. Although these conventional methods give satisfactory estimations, they are prone to large prediction errors due to the inability of their modelling tools to further normalize the nonlinearity in large-noisy fire database. Furthermore, conventional model utilization is not time and economically sustainable, as fire test results integrated with conventional modelling entail a lot of expertise, work and resources. In an attempt to address these challenges, Ref. [14,41] presented estimations for imperative fire properties



from correlation and statistical analysis with comparatively more precise accuracies with less estimation errors than the conventional models.

Due to the rapid improvement of artificial intelligence (AI) technologies in the fire science sector, the shortfalls of the conventional modelling system can be addressed using the ability of AI techniques as an alternative to establishing a generalized normalization within the non-linear database. Research has shown that thermophysical flammability characteristics or parameters can be predicted using machine learning (ML) models in the absence of molecular structures in the modelling process. Algorithm-based machine learning (ML) techniques are currently employed in the fire and flammability science study [16-19] to predict the flammability properties of materials more accurately. Prediction systems based on machine learning generally use learning algorithms with normalized datasets. Artificial neural networks (ANN) [18] are the most commonly used ML method, which has progressively more powerful algorithms to incorporate fire-safety data to validate ML's applicability. This can be attributed to their non-parametric algorithms and capacity to learn and cope with nonlinearities in large-noisy fire data compared to conceptual statistical, correlation, and linear regression methods. Although, this is partly because of the algorithm types used and the constant iterative tuning of network training parameters to achieve the best prediction variable(s). However, the general applicability of ANN is constrained by modelling overfitting, the absence of probabilistic output, and merging at local least points [18].

In Ref. [16], the authors employed MATLAB-developed feedforward backpropagation (FFBP) and generalized regression (GR) neural network model framework to predict HRC, pHRR, THR, pTime, and pTemp of "black" PMMA from quantified sample mass and heating rates of conducted MCC experiments. The work discovered improved HRC-predicted results for PMMA with the lowest error deviations as compared to various conventional estimations in the literature [1, 8, 11]. Hence, showing a superior prediction power over the conventional methods.

To enhance the prediction accurateness of flammability characteristics of PMMA, Ref. [18] developed multivariate adaptive regression splines (MARS) and random forest (RF) models to estimate pHRR, an MCC fire parameter. In their study, sample mass, THR, pTemp, pTime and HRC were found to be marginally sensitive towards the generalized model prediction output of pHRR. However, the results indicated that the heating rate greatly impacted pHRR predictions. In terms of predicting pHRR, MARS outperformed RF with the least RMS statistical errors. A comparative analysis of pHRR prediction results with results of Ref.[16] indicated least mean error deviations of MARS and RF over GR and FFBP models. Other improved ML

systems explored in flammability and thermochemical investigations for prediction purposes include; the least square support vector machine (LSSVM) [42].

The literature has recognized group method of data handling neural network (GMDH-NN) [21-22] and radial basis function neural network (RBF-NN) [23] as improved machine learning models to produce better predictions than the ANN models to explain the shortcomings of ANN for large data predictions. This can be attributed to their powerful algorithms that normalize the nonlinearity in large, noisy datasets for modelling and develop polynomial mathematical equations for parameter estimation of variables. GMDHNN-type applications for parameter estimations in engineering fields include; modeling magnetorheological Damper properties in Ref. [24]. In other works in Ref. [25-26] fused thermal material parameter deposition predictions have been carried out to ascertain GMDH capabilities. Another study also focused on optimizing Stirling engines through the prediction of their thermal parameters respectively. In Ref. [27], the authors studied crested side weirs and modelled their discharge coefficient using the GMDH approach focusing on rectangular shapes, which provided better results. Furthermore, field estimation studies in RBFNN, including Ref. [28], adopted the concept of comparing the prediction prowess of ANN and RB function networks. Their work reported that the RBF model provided a more accurate prediction of combustion parameters for an electrical system optimization than the ANN models.

The present study further enhances THR and HRC predictions of GMDH-type and RBF by incorporating the PMMA MCC flammability data in its model development. The application of GMDH and RBF for predicting PMMA flammability characteristics (THR and HRC) has not yet been explored. For this purpose, the following objectives are sought to be derived from this study: (1) To determine if GMDHNN and RBFNN can be used to predict the MCC characteristics of HRC and THR of PMMA (2) To develop a model equation based on the GMDHNN and RBFNN algorithms for prediction of HRC and THR. (3) To examine the variations in inaccuracy from the flammability predicted parameters by established models. (4) To conduct a comparison between the created models and existing HRC prediction models for PMMA that exist in the literature.

2. Flammability Characteristics

Typically, MCC experimental studies are based on ASTM D7309-13, "Method-A" [7]. MCC test yields flammability characteristics values including; heat release capacity (HRC), peak of heat release rate (pHRR), total heat release (THR), peak of heat release temperature (pTemp or Tmax) and peak of heat release time (pTime). Key parameters, HRC and THR, are therefore expressed in terms of measurable quantities in equations (1)-(2) [7-8].

$$HRC(\eta_c) = \frac{pHRR}{\beta} \quad (1)$$

Where HRC, in (J/g°C) and β = heating rate (K/s), time(t), in seconds. The maximum heat output is expressed as total heat released, THR, in (kJ/g). Peak heat release rate (pHRR) is expressed in W/g.

$HRC(\eta_c)$ is a better indicator of flammability and fire reactivity in a material, often described in combination with temperature stability and combustion characteristic. When complete combustion in an O₂ atmosphere is present, the integral area under the peak HRR curve as a function of time is what is used to calculate THR [5, 7, 29].

3. Materials and Methods

3.1. Material

The material employed in this study is a polymethyl methacrylate (PMMA) with an LOI of 17. The PMMA material was prepared per polymer preparation standards and then used for the fire test. The relevant properties and chemical structure of the PMMA are listed in Table 1.

3.1.1. Material Preparation

Thirty-one (31) pieces from the PMMA sample were sized and cut out using dimensional cutting. Then, the cut-sized PMMA samples were weighed using an analytical semi-micro mettler AX-205 balance, delta range instrument (readability: 0.01 mg, weighing: 81.0 g)[14-29], acquired from Hamilton firm in Nevada, USA. The cut samples were then crushed and milled into powdered form and then utilized for the fire experiment.

3.2. Microscale Combustion Calorimetry (MCC)

The fire experiment was conducted in line with ASTM D7309-13 [7] (Method-A specifications) using PMMA samples. This experiment was performed using a pyrolysis

combustion flow calorimeter (PCFC) or MCC (Govmark manufactured MCC-2 device [31], and Table 2 shows the MCC-2 specifications considered in this study. In the MCC test, the condensed and gas-phase processes of flame combustion are independently recreated by controlled pyrolysis of milligram samples in an inert gas stream and high-temperature thermal oxidation (combustion) of the pyrolyzate in excess oxygen [6], [32] as shown in the flow chart in Fig. 1.

$$THR = \int \frac{pHRR}{t} dt \quad (2)$$

This study utilized the Govmark® technical document, which fundamentally approves sample mass(es) (0.5 - 50 mg) [31]. This study considered nine (9) different constant heating rates (0.1, 0.2, 0.5, 1.0, 1.5, 2.0, 2.5, 3.0, 3.5 K s⁻¹) [18] based on the experimental designed values. Then, three (3) replicas of each of the thirty-one (31) cut-out PMMA sample masses (1-3.5 mg) were prepared. The pyrolyzer and combustor were adjusted at 75-600°C and 900°C, respectively, to heat the PMMA samples. The oxygen flow rate and concentration in gases leaving the combustion chamber were continuously measured. At a point, the thermally degraded material then discharged heated gases into the combustion chamber, where they were mixed with oxygen to complete the oxidation process. Next, nitrogen was used to propel these heated gases into the chamber.

Each sample was put to the test in three (3) turns of firing. Usually, the heat emission of the PMMA samples is directly correlated with the oxygen consumption principle. The mean of three (3) measurements was taken for each of the MCC characteristics listed in ASTM D7309-13 [7], including the peak of heat release rate (pHRR), the peak of heat release duration, heat release capacity (HRC), total heat released (THR), and heat release temperature.

Table 1. Structure and properties of PMMA [16, 17, 29]

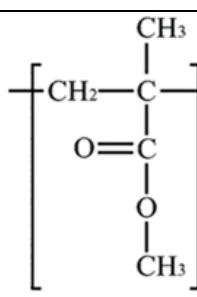
Compound	Molecular formula	Chemical structure	ρ /(Kg/m)	k /(W/mK)	c /(J/gK)	LOI (%)
PMMA	$[(C_5 H_8 O_2)_n]$		1.180	0.185	1.510	17
LOI-Limiting Oxygen Index, c -Specific heat, ρ -Density, k -Thermal conductivity [33].						

Table 2. Govmark manufactured MCC-2 experimental device specifications

Specifications	Range
Sample heating rate	(0-10 K/s)
Gas flow rate	50-200 cm ³ /min, response time of < 0.1 s, sensitivity of 0.1% of full-scale
Repeatability	(± 0.2%) of full scale and accuracy of ± 1% of full-scale deflection
Sample size	0.50-50.0 mg (milligrams).
Detection limit	5.0 mW.
Repeatability	(± 2%, 10 mg specimen)

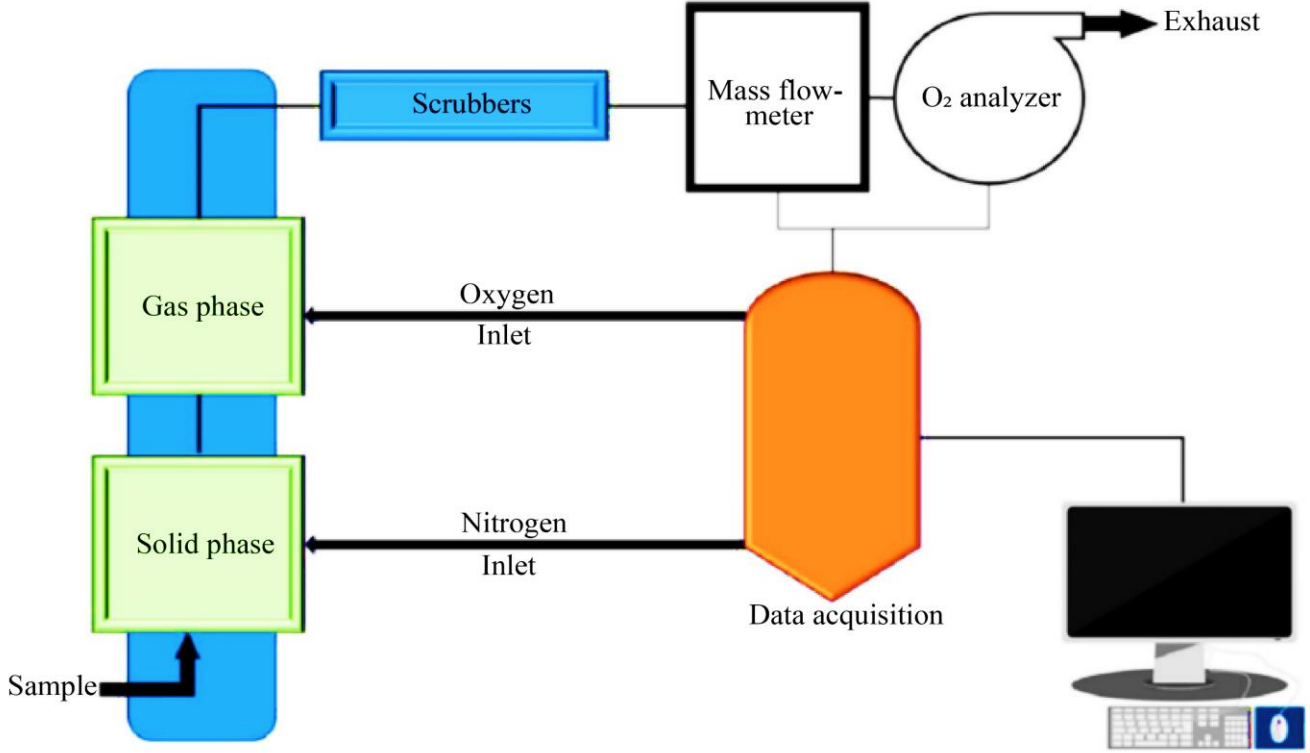


Fig. 1 Setup of MCC or Pyrolysis-Combustion flow calorimeter (PCFC) [5]

3.3. Group Method of Data Handling-Type Neural Network (GMDHNN)

A supervised machine learning approach, known as the group method of data handling (GMDH), was first presented by [21]. Additionally, GMDH is a family of algorithms distinguished by an inductive self-organizing process and a method for sorting out data to automatically develop networks suitable for the noise level within the dataset [22, 34].

An essential component of GMDHNN is a two-variable quadratic polynomial that models nonlinear systems using NN networks as a data-driven model. In contrast to typical neural networks, no initial parameter assumptions such as activation function and the predetermined network structure are required, hence representing a better neuron architecture that minimizes prediction errors during training [35]. For this purpose, assuming a training set *z* of *n* number of parameters and having a variable input range of (x_1, \dots, x_p) and an

output *y* which is expressed to be HRC or THR, in this study. GMDHNN develops a neuron network for modelling function *f* as a polynomial function, represented in Equation (3): [21, 22]]:

$$y = f(x_1, \dots, x_p) \tag{3}$$

The Volterra *f* function describes the relation of inputs to outputs. This function can be represented as a discrete analog of the Kolmogorov-Gabor polynomial by means of the input variables [36], as stated in Equation (4).

$$y = a_0 + \sum_{i=1}^p a_i x_i + \sum_{i=1}^p \sum_{j=1}^p a_{ij} x_i x_j + \sum_{i=1}^p \sum_{i=1}^p \sum_{k=1}^p a_{ijk} x_i x_j x_k \tag{4}$$

Since the difficulty of the polynomial increases with the number of input variables, GMDHNN chooses an ideal number of input variables that best describe the output variable *y* to attain the best degrees (only part)—a typical

schematic architecture of a multi-entry GMDH network illustrated in Figure 2.

For the GMDH network in this experimental study, each neuron contains two (2) inputs and only a single output. The output for each neuron is estimated by means of Ivakhnenko's polynomial mentioned in Equation (5):

$$y = a_0 + a_1x_i + a_2x_j + ax_ix_j + a_4x_i^2 + a_5x_j^2 \quad (5)$$

where; $a_i(i=0,1,2,3\dots, n)$ the weights of the neurons [35].

In order to obtain the sets with the lowest mean squared errors (MSE), neuron weights are continuously adjusted during the training of GMDHNN networks. Parameters for each layer in the GMDHNN model must be estimated using the ordinary least square method. The model's layer count is increased up until it reaches the least MSE or a particular selection criteria level. When modeling, GMDH uses the symmetry, unbiasedness, or balance-of-variables measure. Symmetry or regularity criteria is calculated using Equation (6) [34, 35].

$$R_{l,m} = \sqrt{\frac{\sum_{k=1}^N (y_k - w_k)^2}{\sum_{k=1}^N (y_k)^2}} \quad (6)$$

Where: y_k denotes the desired target value (measured experiment data), and w_k denotes the predicted output parameter with feature vectors; m th neuron of l th layer for the k th parameter. A selection decision is reached considering the range of values T_l of $R_{l,m}$, which includes the minimum ($R_{l,min}$) and the maximum ($R_{l,max}$) as shown in Equation (7) [37]:

$$T_l = \beta(R_{l,max}) + (1 - \beta)(R_{l,min}) \quad (7)$$

With β as the normalized input data (x_i) between 0 and 1. The layer with the least error is then selected to be the output network layer.

3.4. Radial Basis Function Neural Network (RBFNN)

Input, hidden, and output layers for the radial basis function neural network (RBFNN) [28] are basically linked to perform network-supervised training. Fig. 3 illustrates a typical RBFN topology architectural network with n - entries, l hidden units and m output layers.

Using unweighted connections, the RBFNN input layer assigns data into the hidden layer space and the system network. The hidden layer then uses a nonlinear function to modify the entry data. Each neuron calculates a Euclidean norm in the hidden layer, representing the separation between entering the network and localizing the neuron's centre. Activation of the neuron is then calculated and outputted by a radial basis activation function [37].

The Gaussian activation function [38] was used from input to hidden through to the output layer computations of the RBFN network in this study.

Assuming an RBFN network with n inputs, l hidden units, and m outputs (HRC or THR), the output layer calculation can be computed. In the process of activating the input of hidden unit l , using input vector $x_{i,\dots,n}$ ($i = 1, 2, n$) is weighted by input weights w^h and expressed in Equation (8) as [28, 39]:

$$I_l = \{x_1w_{1,l}^h, x_2w_{2,l}^h, \dots, x_nw_{n,l}^h\} \quad (8)$$

Given that;

x_n is the n -th input, $w_{n,l}^h$ as the input weight between input n and hidden unit l . where, n is the index of input and l is the index of hidden units. Generally, all input weights are set at unity "1". In estimating to compute the hidden layer, the output of hidden unit l is calculated from Equation (9) [39]:

$$\phi_l(I_l) = \exp\left(-\frac{\|I_l - C_l\|^2}{2\sigma_l^2}\right) \quad (9)$$

Where, activation function $\phi_l(I_l)$ for hidden unit l is chosen as the Gaussian function, and C_l denoting center of hidden unit l of the Gaussian function. σ_l as the width or spread parameter of the Gaussian bells of hidden unit l . Let y_m denote the output of the m th radial basis function on the i th sample. Each output target node l is computed using the weights $w_{l,m}^o$ [28]. Hence, estimating the output layer computation, the m output network can be calculated, expressed in Equation (10) as [28, 39]:

$$y_m = \sum_{l=1}^L \phi_l(I_l)w_{l,m}^o + w_{0,m}^o \quad (10)$$

Given; $w_{l,m}^o$, output weight between hidden unit l and output unit m ; m is the index of output; $w_{0,m}^o$ bias weight of output unit m . Generally, the output layer contains the linear function and uses the weighted sum of the hidden layer as the propagation function [28]. From Eqs. (8-10), four parameters, such as input weight matrix w^h , output weights matrix w^o , center matrix C and width vector σ , are key in algorithm computation. Usually, after setting input weights to "1", linear least squares (LLS) approaches are employed to adjust the output weights for nonlinearities. Iteratively LS method [38] improves the nonlinear performance of the output layer. Offering optimum minimum-normal approximation of the inverse in the least-medium-square direction. This training process continues until the network error reaches an acceptable value [28, 39].

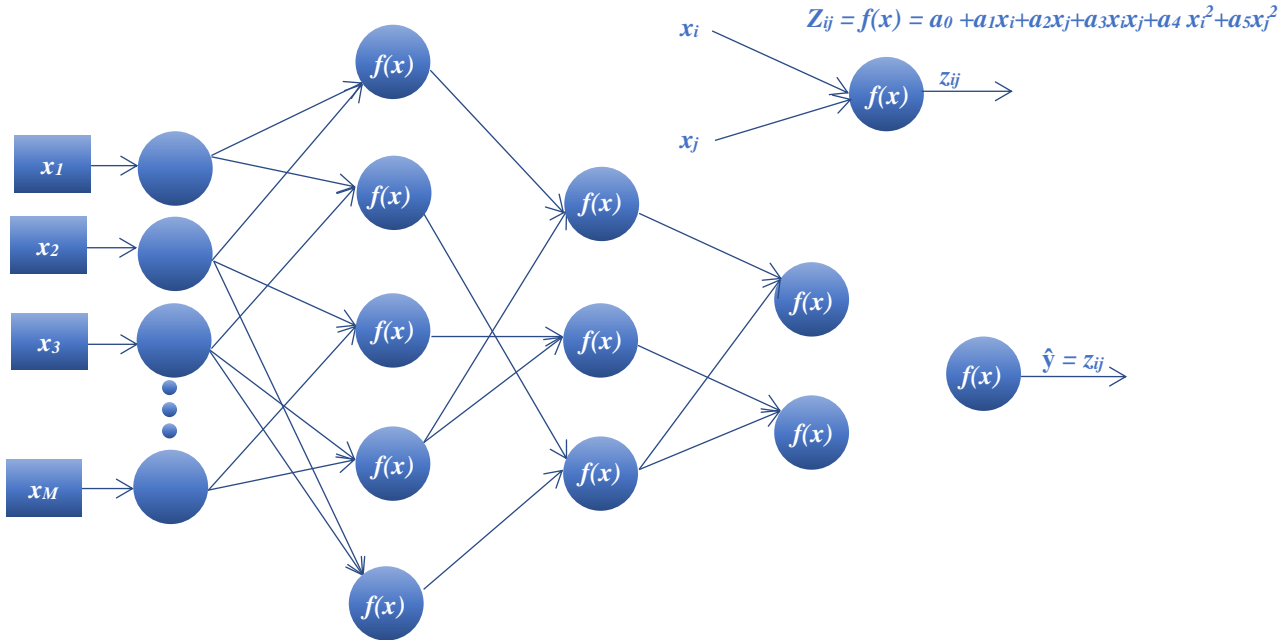


Fig. 2 A typical architecture of a multi-inputs GMDH networks with one (1) output [22]

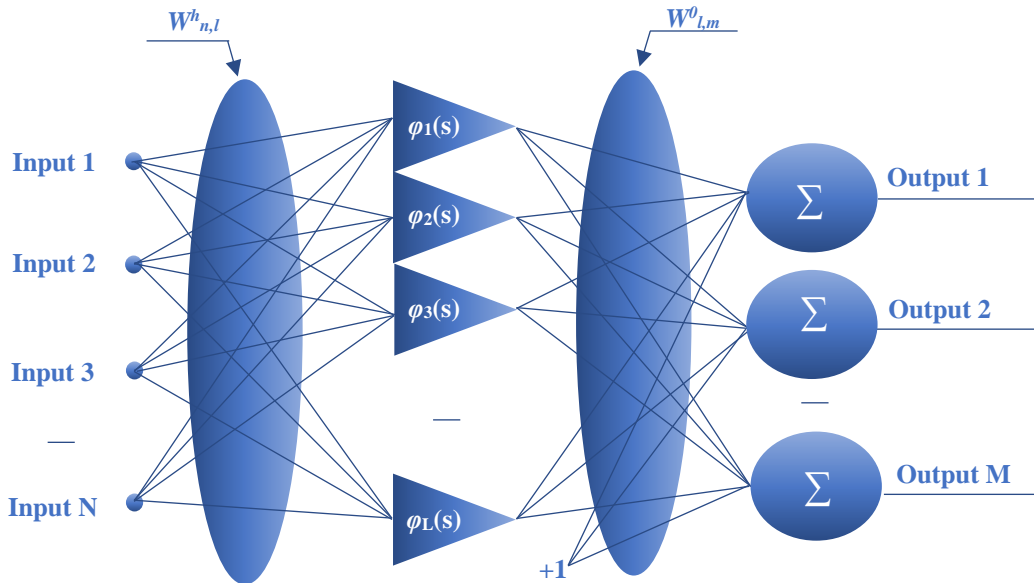


Fig. 3 Typical RBFNN architecture [28]

3.5. Models Implementation

The main objective of this study is to develop prediction models to estimate THR and HRC flammability parameters of PMMA from MCC fire tests using neural network (NN) approaches. Two input parameters were used for the GMDHNN and RBFNN models development. The sample mass (m) and heating rate (β) were employed through inputs or independent parameters to predict the study's dependent variables, total heat release and heat release capacity. Subsequently, the MCC's data was then

arbitrarily split into training then testing sets for these models' development. The training set was used to alter the algorithm [40]. This method is carried out using a hold-out cross-validation technique. In order to prevent overfitting, the correct amount of data is used when training NN algorithms. The fraction utilized as training data must, therefore, accurately parametrize the entire set of data [23].

In other words, the testing set consisted of 4 (15%) out of the MCC dataset, whereas 27 out of the 31 MCC data, or

85%, were randomly selected to make up for the training set. Training and testing datasets used to build the models are shown in Table 3. The models were implemented using MATLAB (R2018a version, MathWorks Inc., Natick, MA, USA). The RBFNN used the Gaussian activation function in the modelling for normalizing the data between (- 1 and 1). In contrast, the Levenberg-Marquardt algorithm was used in this study to train RBFNN partitioned data. The process of successive trial and error helped to produce the best outcome. The ideal model network topology was determined to achieve the highest correlation coefficient (R) after several try-and-error of training [19].

3.6. Data Normalization

Data set normalization is a process that is used to train the neural network to ensure that the data set is consistent with the model's variability. Usually, the data set is normalized to a certain interval as [-1, 1], [0, 1] or another scaling parameter to ensure constant variability in the RBF and GMDH models. By speeding up convergence, this data standardization lowers the likelihood of reaching local minima. The splitted input and output variables in this investigation were standardized to the range [-1, 1] using Equation (11): [23], [38].

$$y_i = y_{min} + \frac{(y_{max} - y_{min}) \times (x_i - x_{min})}{(x_{max} - x_{min})} \quad (11)$$

where x_i is the measured experimental data, and y_i is the normalized data. While x_{min} and x_{max} represent the minimum and maximum experimental data values with y_{max} and y_{min} set to 1 and -1, respectively.

3.7. Models Performance Indicators

The effectiveness of RBFNN and GMDHNN models on training and testing data was evaluated in this work using a variety of statistical valuation measures. This study aimed to estimate the performance of the RBFNN and GMDHNN models in terms of training and testing data to compare the experimentally determined training and testing data values of GMDHNN, and RBFNN predicted data. To do so, various statistical indicators were used.

These included root mean squared error (RMSE), the mean absolute error (MAE), the coefficient of determination (R^2), and the correlation coefficient (R). The root of the mean square error, or RMSE, quantifies the discrepancy between experimental outcomes and predicted data. Also, the MAE is an average absolute difference between the measured and predicted data. As MAE and RMSE values get lower, the better accuracy of the prediction [40]. Additionally, the correlation coefficient and the coefficient of determination are two of the most common tools used to measure the relationship between experimental and predicted results. The

former shows how much variability exists in the study's results, while the latter describes the extent to which the predicted results can explain the variance. When R and R^2 values are closer to 1, there is a more significant linear relationship between the two variables. Equations (12)-(15) presents the various statistical indicators [16,40]:

$$R = \frac{\sum_{i=1}^n (e_i - \bar{e})(p_i - \bar{p})}{\sqrt{\sum_{i=1}^n (e_i - \bar{e})^2 \times \sum_{i=1}^n (p_i - \bar{p})^2}} \quad (12)$$

$$R^2 = \left(\frac{\sum_{i=1}^n (e_i - \bar{e})(p_i - \bar{p})}{\sqrt{\sum_{i=1}^n (e_i - \bar{e})^2 \times \sum_{i=1}^n (p_i - \bar{p})^2}} \right)^2 \quad (13)$$

$$RMSE = \sqrt{\frac{1}{n} \sum_{i=1}^n (e_i - p_i)^2} \quad (14)$$

$$MAE = \frac{1}{n} \sum_{i=1}^n |e_i - p_i| \quad (15)$$

$$\bar{e} = \frac{1}{n} \sum_{i=1}^n e_i \quad (16)$$

With reference to Eqs. (12 – 15) [16]; n = total number of experimental data, while i = an integer varying from 1 to n . e_i = measured value, p_i = predicted value, \bar{e} = mean measured value and \bar{p} = mean predicted value.

4. Results and Discussion

4.1. MCC Experiment Results

Statistical descriptions for MCC parameters obtained for the thirty-one sample masses used in this study are detailed in Ref. [18].

Fig. 4(a) illustrates a plot of specific HRR against associated temperatures from the measured MCC experimental dataset. The curves in the graph depict the thirty-one (31) heating rates considered in the experiments and range from (0.1-3.5 K/s). The curves demonstrate that, for various tested sample masses of PMMA, increasing heating rates increase both the peak HRR and peak temperatures (pTemp), respectively [17-18, 32, 33].

Table 3. RBFNN and GMDHNN models training/testing data

Inputs		Outputs	
β (K/s)	Mass (mg)	HRC (J/g °C)	THR (kJ/g)
Training Data			
0.1	1.09	750.9±0.5	15.3±0.8
0.1	1.47	636.5±0.7	10.2±1.9
0.1	2.58	918.5±0.8	18.6±0.9
0.2	1.1	804.3±0.4	20.6±0.3
0.2	1.61	756.9±1.5	21.7±3.6
0.2	2.6	776.5±0.5	26.2±3.8
0.5	1.06	615±0.4	26.7±2.7
0.5	1.67	598.5±1	26.5±0.4
0.5	2.57	630.1±0.6	27.8±1.1
1	1.06	534.2±0.6	31.8±0.5
1	1.48	489±1.6	28.1±0.3
1	2.68	475.6±0.9	28.8±0.9
1.5	1.06	403.5±1.3	28.9±0.5
1.5	1.54	416.5±1.2	29.4±0.8
1.5	2.56	447.9±1.7	28.9±0.3
2	1.06	442.6±0.7	30.7±1.3
2	1.54	438.5±0.9	31.2±0.6
2	2.59	387.2±1.2	29.2±0.4
2.5	1.1	404.5±1.1	30.9±1.4
2.5	1.55	395.3±0.6	29.3±2.1
2.5	2.51	340.4±2	29.7±0.8
3	1.03	373.7±0.7	30.3±0.7
3	1.06	385.4±0.7	30.3±0.1
3	1.5	375.2±0.8	30.4±0.3
3.5	0.99	345.5±2.1	31.3±0.6
3.5	1.67	344.5±0.8	30.3±3
3.5	3.46	320.3±1.7	29.6±1.1
Testing Data			
0.1	1.79	537.6±0.9	11.2±0.1
0.2	1.75	659.5±0.8	19.2±1
3	2.64	342.2±1.2	29.8±0.9
3.5	2.72	365.4±1.3	31.1±0.4

Similarly, measurements and observations of the impact of sample mass on pHRR proved that, for almost all measured heating rates, the pHRR values reported on average for the 1 mg sample mass were the highest, as illustrated in Fig. 4(b).

That is to say, a smaller sample mass specimen, when subjected to fire, tends to produce higher pHRR values at lower pyrolysis temperature and time [32].

4.2. RBFNN Prediction Results

This section analysed the predicted outputs from the RBF neural network MATLAB developed a model for THR and HRC estimation. The training and testing results obtained in Fig. 5 and 6, respectively, showed that the RBFNN produced THR and HRC estimates having very high R and R² with low errors of MSE.

In addition, Cross-plots in Fig. (7 – 10) further interpret the experimental results versus measured findings for the training and testing datasets. The best prediction from Fig. (7 and 8) with the least errors was revealed through THR training. The lines of best fit for the HRC training and test results, respectively, were not very well fitted with the data points, as shown in Figures 9 and 10.

Even though both neural network models delivered excellent predictions with the least error rates that are highly correlated with measured data, the prediction of THR, thus, produced superior R and lower RMSE values compared to the results of HRC.

It can be observed that the RBFNN model's prediction of the THR training and testing data displays outstanding agreement with the measured data since its fit line is more closely aligned with the ideal line than the fit line of the HRC model.

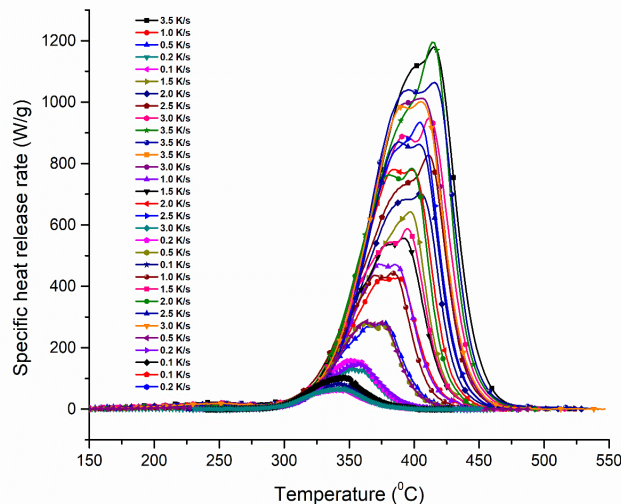


Fig. 4 (a) Plot of specific HRR against the temperature of MCC dataset for PMMA

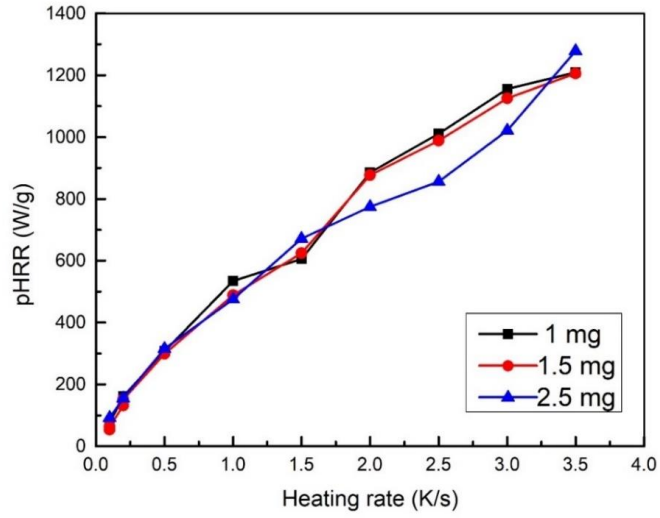


Fig. 4 (b) Sample mass effect on peak heat release rate (pHRR)

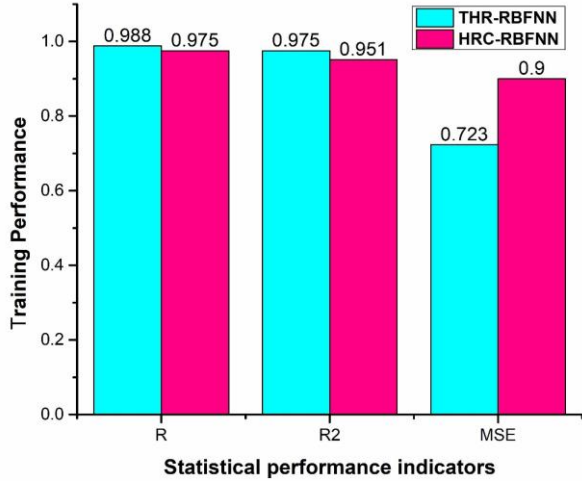


Fig. 5 Performance of THR-RBFNN and HRC-RBFNN during training

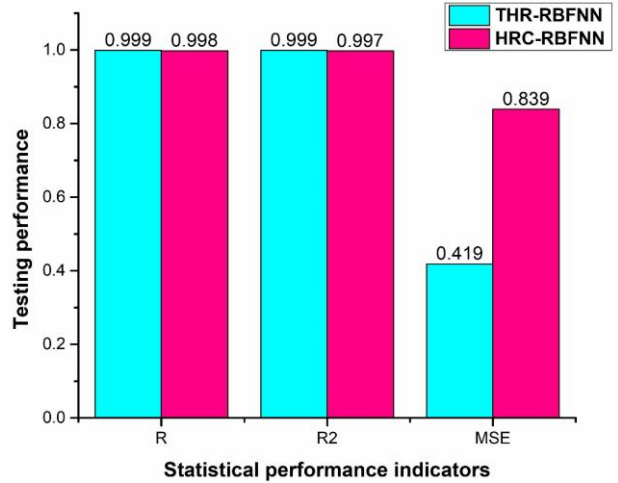


Fig. 6 Performance of THR-RBFNN and HRC-RBFNN during testing

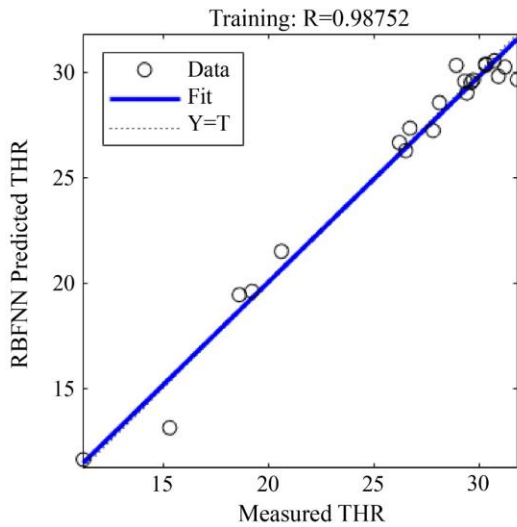


Fig. 7 RBFNN-training predicted THR versus experimental THR

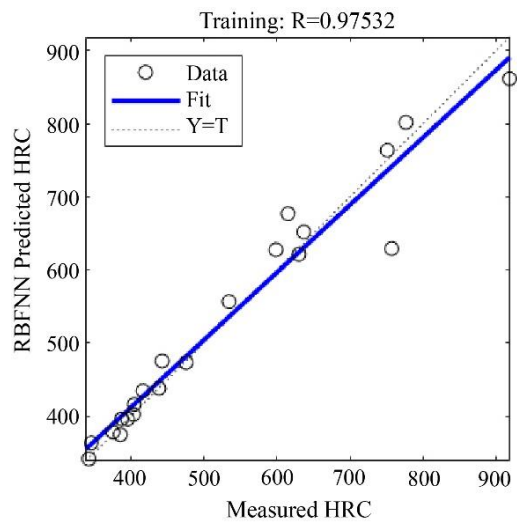


Fig. 8 RBFNN-training predicted HRC versus experimental HRC

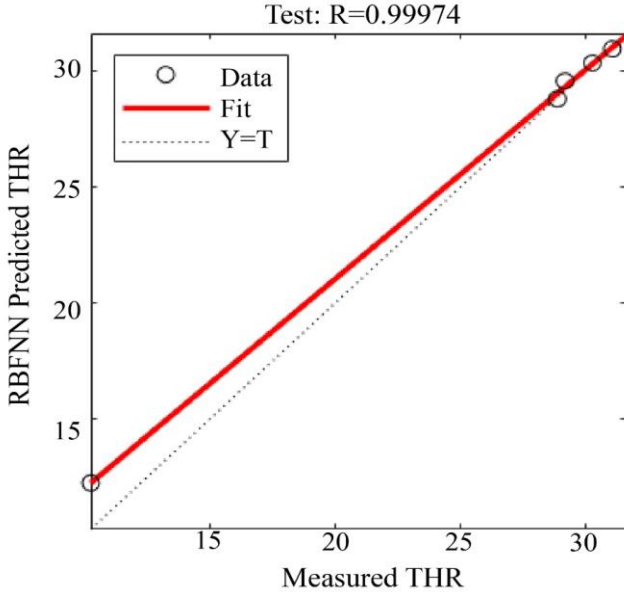


Fig. 9 RBFNN-testing predicted THR versus experimental THR

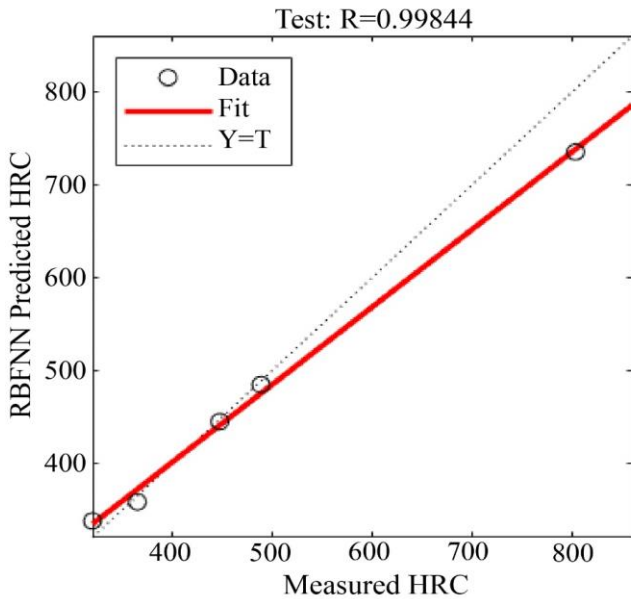


Fig. 10 RBFNN-testing predicted HRC versus experimental HRC

4.3. GMDHNN Prediction Results

Similarly, results from predicted outputs from the GMDH-type neural network model (developed in MATLAB) were analysed for THR and HRC estimation. The training and testing results obtained in Fig. 11 and 12, respectively, showed that the GMDHNN produced THR and HRC estimates having very high R and R² with low errors of MSE.

Fig. (11 and 12) displays the results for the performance indicators from the neural network models. The exceptional predictability of the created model is backed up by the R, R², MAE, and MSE values for training and testing. The analysis

of the training data for HRC revealed that the predictions made by GMDHNN had a very high correlation to the findings of the measurements. It is evident that the training strategy used for the HRC model produced the highest R and R² values (0.9999) and the least MSE and MAE values. Again, Fig. (11 and 12) shows that, on average, MAE and MSE offer a low error margin that is steady over the course of the model's performance.

In addition to the aforementioned results, Fig. (13 – 16) demonstrates experimentally measured and predicted HRC and THR results. After training, the predicted data values were found to be in perfect agreement with the experimental results (dataset), as can be seen by carefully examining the cross-plot results of Fig. (13 – 16)). The training results showed that the HRC model had greater predictive power over the THR model going forward. This was not entirely the case, though, as GMDH prediction of THR had a marginally stronger correlation with the measured THR values.

Generally, the GMDH neural network model system in predicting HRC of PMMA with inputs parameters, *mass* and β generated mathematical equations for obtaining this MCC parameter. Representation of the modelling equation is presented in Equation (17):

$$HRC \left(\frac{J}{g^{\circ}C} \right) = -23.5428 + 11.387(mass) + 1.00591(X^1) \tag{17}$$

$$X^1 = 752.565 - 265.323(\beta) - 6.05114(\beta)(mass) + 47.5798\beta^2$$

Equation (18) was equally derived for predicting THR from sample mass (m) and heating rate (β):

$$THR \left(\frac{kJ}{g} \right) = 20.8568 + 0.121466(mass) + 3.37651\beta \tag{18}$$

Despite the marginal insignificant variations in R, R² and MSE values obtained for both models. RBFNN and GMDHNN's prediction accuracy showed workable models with acceptable correlation coefficients, mean averages, and minimal root mean squared errors. Nonetheless, GMDHNN modeling for HRC prediction was more precise. In terms of predicting the flammability properties of a polymethyl methacrylate, GMDHNN fared better than RBFNN generally.

A comparative assessment of the testing performance of the GMDHNN and RBFNN and how the estimations deviate from measured HRC is demonstrated in Fig. 17. From Fig. 17, it can be deduced that there was a better improvement in the generalization test of the models once the dataset incorporated into the estimation of HRC is normalized.

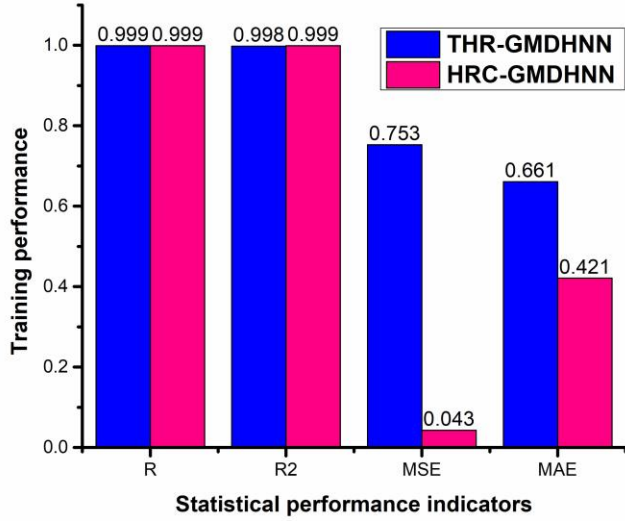


Fig. 11 Performance of THR-RBFNN and HRC-RBFNN during training

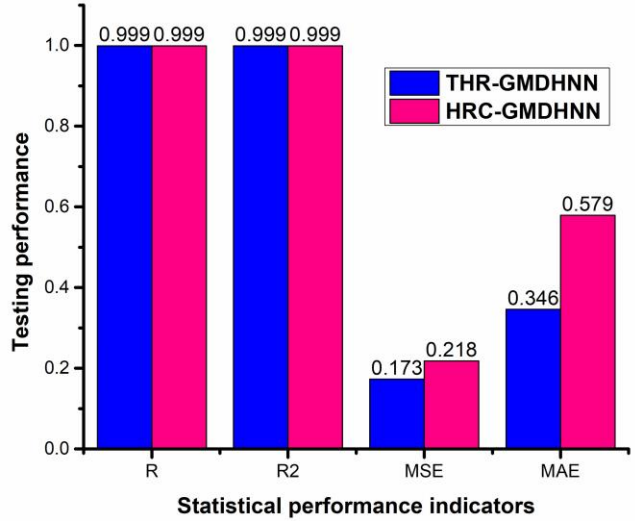


Fig. 12 Performance of THR-RBFNN and HRC-RBFNN during testing

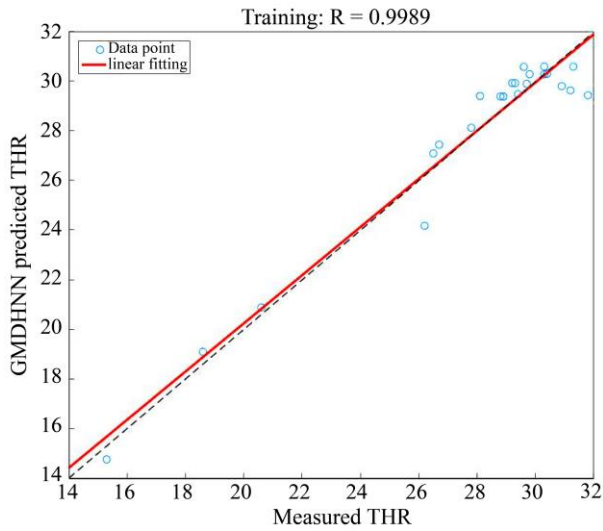


Fig. 13 GMDHNN-training predicted THR versus Experimental THR

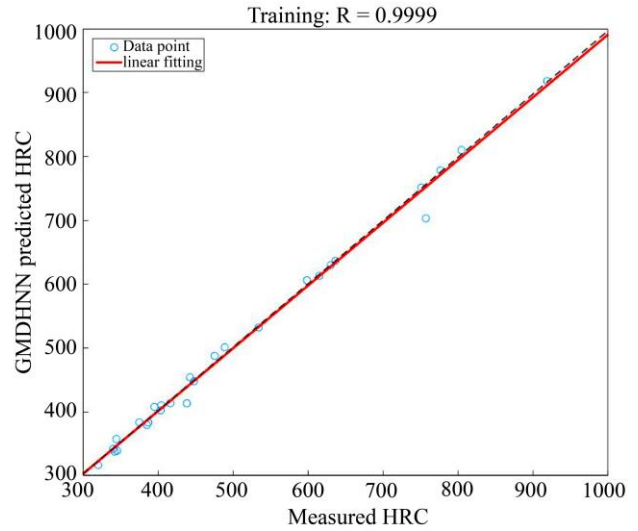


Fig. 15 GMDHNN-training predicted HRC versus Experimental HRC

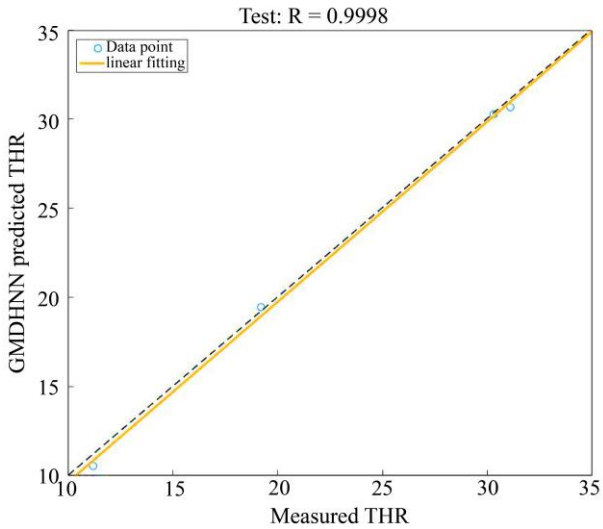


Fig. 14 GMDHNN-testing predicted THR versus Experimental THR

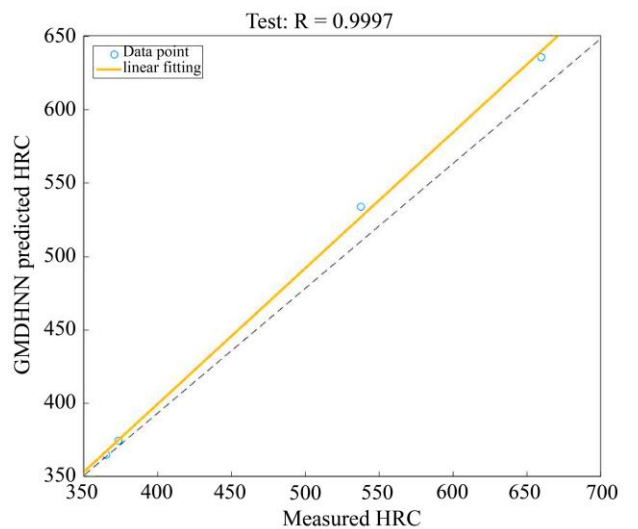


Fig. 16 GMDHNN-testing predicted HRC versus Experimental HRC

4.4. Comparison Analysis with other HRC Models

The HRC data used in the study were then compared with the mean HRC values produced from other PMMA results from the literature in Ref. [1, 11, 16]. The core idea was to determine the predictive prowess of GMDHNN and RBFNN against the models in Ref. [1, 11, 16]. From a comparative analysis of the difference from their measured and predicted mean HRC outcomes, as illustrated in Fig. 18, we can infer that the GMDHNN prediction outcomes had the least deviation of mean HRC outcome, indicating a high level of accuracy, with an error deviation of a 1.32 for PMMA. This affirms GMDHNN-type as a highly applicable system in providing PMMA flammability characteristics HRC estimations for polymers' development of flame-retardant properties.

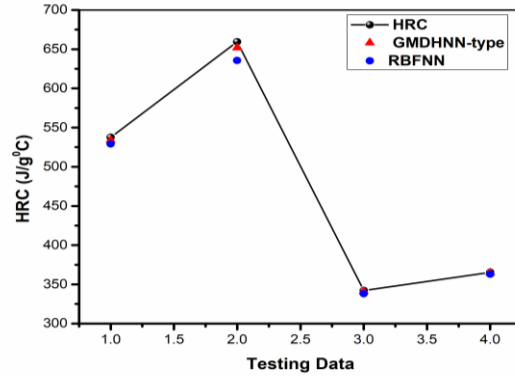


Fig. 17 Comparing the testing results of the GMDHNN, RBFNN and MCC-HRC data

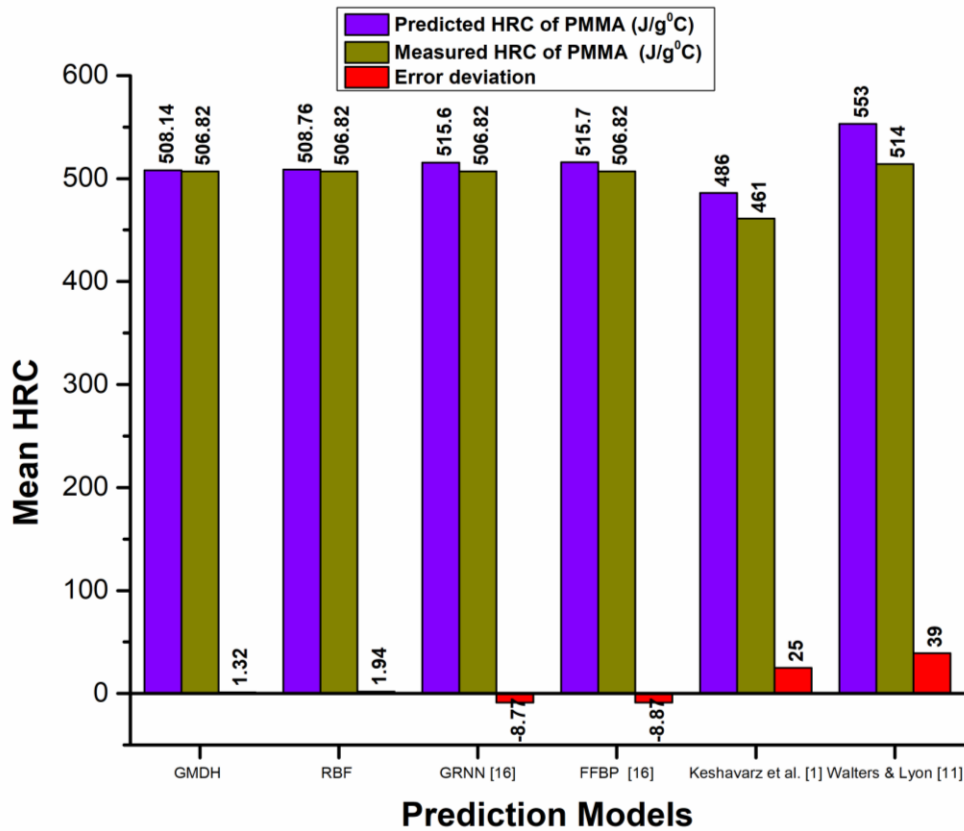


Fig. 18 Mean HRC values of RBFNN and GMDHNN compared to other literature models

5. Conclusion

In this study, RBF and GMDH neural networks were developed and applied to model the flammability characteristics of polymethyl methacrylate as determined by the MCC fire test. Using the sample mass and corresponding heating rates as input parameters, the experiment's test findings were used to estimate heat release capacity and total heat released. With sample mass and heating rate as input variables, this work developed an artificial intelligence-

supervised machine learning model based on RBFNN and GMDHNN for predicting HRC and THR. Although GMDHNN outperformed RBFNN in predicting HRC, it was discovered that both models exhibited excellent repeatability with nominal errors and excellent agreement with measured experimental data. Moreover, compared to GMDHNN, RBFNN achieved values with greater correlation when estimating THR; as a result, RBFNN performed relatively better when predicting THR.

The mean value of the predicted HRC from the current neural network models was then compared to the PMMA results from other existing flammability estimation and predictive modeling techniques in the literature to ascertain the error margins with the models' predictive power. The results indicate that GMDHNN offered the lowest error deviation for predicting PMMA amongst the predicted models

in the literature, followed by RBFNN. Hence, compared to GMDH, RBFNN had an error deviation of 1.94 as against 1.32 for GMDHNN. Therefore, this study demonstrates that the GMDHNN and RBFNN models are capable of accurately predicting the PMMA flammability parameters from the MCC fire-safety test with minimal prediction errors.

References

- [1] Mohammad Hossein Keshavarz et al., "A Simple Model for Reliable Prediction of the Specific Heat Release Capacity of Polymers as an Important Characteristic of their Flammability," *Journal of Thermal Analysis and Calorimetry*, vol. 128, no. 1, pp. 417–426, 2017. [[CrossRef](#)] [[Google Scholar](#)] [[Publisher Link](#)]
- [2] N. Saba et al., "A Review on Flammability of Epoxy Polymer, Cellulosic and Non-Cellulosic Fiber Reinforced Epoxy Composites," *Polymers Advanced Technologies*, vol. 27, no. 5, pp. 577–590, 2016. [[CrossRef](#)] [[Google Scholar](#)] [[Publisher Link](#)]
- [3] H. E. Yang, "Quantitative Microscale Assessment of Polymer Flammability," *Plastics Research*, 2015. [[Google Scholar](#)]
- [4] Richard Norman Walters, "Development of Instrumental and Computational Tools for Investigation of Polymer Flammability," Universities of Central Lancashire, p. 267, 2013. [[Google Scholar](#)] [[Publisher Link](#)]
- [5] Qiang Xu et al., "A Critical Review of the Methods and Applications of Microscale Combustion Calorimetry for Material Flammability Assessment," *Journal of Thermal Analysis and Calorimetry*, vol. 147, no. 11, pp. 6001–6013, 2022. [[CrossRef](#)] [[Google Scholar](#)] [[Publisher Link](#)]
- [6] R. E. Lyon et al., "Principles and Practice of Microscale Combustion Calorimetry," *Fed. Aviat. Adm. Atl. City Airport, NJ 8405*, pp. 1–80, 2013.
- [7] "Standard Test Method for Determining Flammability Characteristics of Plastics and Other Solid Materials Using Microscale Combustion Calorimetry," *ASTM D7309, American Society for Testing and Materials, West Conshohocken, PA*, pp. 1–11, 2013. [[CrossRef](#)] [[Google Scholar](#)] [[Publisher Link](#)]
- [8] Richard E. Lyon et al., "A Molecular Basis for Polymer Flammability," *Polymer (Guildf)*, vol. 50, no. 12, pp. 2608–2617, 2009. [[CrossRef](#)] [[Google Scholar](#)] [[Publisher Link](#)]
- [9] Fariborz Atabaki, and Mohammad Hossein Keshavarz, "The Simplest Model for Reliable Prediction of the Total Heat Release of Polymers for Assessment of their Combustion Properties," *Journal of Thermal Analysis and Calorimetry*, 2017. [[CrossRef](#)] [[Google Scholar](#)] [[Publisher Link](#)]
- [10] Priya V. Parandekar, Andrea R. Browning, and Om Prakash, "Modeling the Flammability Characteristics of Polymers using Quantitative Structure – Property Relationships (QSPR)," *Polymer Engineering and Science*, vol. 55, no. 2, pp. 1553–1559, 2015. [[CrossRef](#)] [[Google Scholar](#)] [[Publisher Link](#)]
- [11] Richard N. Walters, and Richard E. Lyon, "Molar Group Contributions to Polymer Flammability," *Journal of Applied Polymer Science*, vol. 87, no. 3, pp. 548–563, 2003. [[CrossRef](#)] [[Google Scholar](#)] [[Publisher Link](#)]
- [12] R. Sonnier et al., "Relationships between the Molecular Structure and the Flammability of Polymers : Study of Phosphonate Functions using Microscale Combustion Calorimeter," *Polymer (Guildf)*, vol. 53, no. 6, pp. 1258–1266, 2012. [[CrossRef](#)] [[Google Scholar](#)] [[Publisher Link](#)]
- [13] Rodolphe Sonnier et al., "Prediction of Thermosets Flammability using a Model based on Group Contributions," *Polymer (Guildf)*, vol. 127, pp. 203–213, 2017. [[CrossRef](#)] [[Google Scholar](#)] [[Publisher Link](#)]
- [14] Rhoda Afriyie Mensah et al., "Correlation Analysis of Cone Calorimetry and Microscale Combustion Calorimetry Experiments Correlation Analysis of Cone Calorimetry and Microscale Combustion Calorimetry Experiments," *Journal of Thermal Analysis and Calorimetry*, vol. 136, pp. 589–599, 2018. [[CrossRef](#)] [[Google Scholar](#)] [[Publisher Link](#)]
- [15] R.Swarnalatha et al., "Synthesis, Characterization, and Dielectric Studies of (1-x) PMMA: x PC: 10PVP: 5LiClO4 Plasticized Blend Polymer Solid Electrolyte Systems," *SSRG International Journal of Material Science and Engineering*, vol. 6, no. 3, pp. 1–4, 2020. [[CrossRef](#)] [[Publisher Link](#)]
- [16] Solomon Asante-Okyere et al., "Generalized Regression and Feed Forward Back Propagation Neural Networks in Modelling Flammability Characteristics of Polymethyl Methacrylate (PMMA)," *Thermochimica Acta*, vol. 667, pp. 79–92, 2018. [[CrossRef](#)] [[Google Scholar](#)] [[Publisher Link](#)]
- [17] Rhoda Afriyie Mensah et al., "Application of Adaptive Neuro-Fuzzy Inference System in Flammability Parameter Prediction," *Polymers (Basel)*, vol. 12, no. 1, p. 122, 2020. [[CrossRef](#)] [[Google Scholar](#)] [[Publisher Link](#)]
- [18] Mohammed Okoe Alhassan et al., "Novel Approaches to Modelling Flammability Characteristics of Polymethyl Methacrylate (PMMA) via Multivariate Adaptive Regression Splines and Random Forest Methods," *Asian Journal of Research in Computer Science*, vol. 4, no. 4, pp. 1–14, 2020. [[CrossRef](#)] [[Google Scholar](#)] [[Publisher Link](#)]

- [19] Rhoda Afriyie Mensah et al., “Comparative Evaluation of the Predictability of Neural Network Methods on the Flammability Characteristics of Extruded Polystyrene from Microscale Combustion Calorimetry,” *Journal of Thermal Analysis and Calorimetry*, vol. 138, pp. 3055-3064, 2019. [[CrossRef](#)] [[Google Scholar](#)] [[Publisher Link](#)]
- [20] Jitesh J. Shewale, and Kiran S. Bhole, "Fabrication and Analysis of Three Dimensional Polymer Microneedle Array Potentially for Transdermal Drug Delivery," *SSRG International Journal of Mechanical Engineering*, vol. 2, no. 2, pp. 22-27, 2015. [[CrossRef](#)] [[Google Scholar](#)] [[Publisher Link](#)]
- [21] A. G. Ivakhnenko, “Polynomial Theory of Complex Systems,” *IEEE Transactions on Systems, Man, and Cybernetics*, vol. 1, no. 4, pp. 364–378, 1971. [[CrossRef](#)] [[Google Scholar](#)] [[Publisher Link](#)]
- [22] Saeb M. Besarati et al., “Modeling Friction Factor in Pipeline Flow Using a GMDH-Type Neural Network,” *Cogent Engineering*, vol. 2, no. 1, 2015. [[CrossRef](#)] [[Google Scholar](#)] [[Publisher Link](#)]
- [23] Yao Yevenyo Ziggah et al., “Capability` of Artificial Neural Network for Forward Conversion of Geodetic Coordinates (ϕ, λ, h) to Cartesian Coordinates (X, Y, Z),” *Mathematical Geosciences*, vol. 48, no. 6, pp. 687–721, 2016. [[CrossRef](#)] [[Google Scholar](#)] [[Publisher Link](#)]
- [24] Khaled Assaleh, Tamer Shanableh, and Yasmin Abu Kheil, “Group Method of Data Handling for Modeling Magnetorheological Dampers,” *Intelligent Control and Automation*, vol. 4, no. 1, pp. 70–79, 2013. [[CrossRef](#)] [[Google Scholar](#)] [[Publisher Link](#)]
- [25] Farzad Rayegani, and Godfrey C. Onwubolu, “Fused Deposition Modelling (FDM) Process Parameter Prediction and Optimization using Group Method for Data Handling (Gmdh) and Differential Evolution (DE),” *The International Journal of Advanced Manufacturing Technology*, vol. 73, no. 1–4, pp. 509–519, 2014. [[CrossRef](#)] [[Google Scholar](#)] [[Publisher Link](#)]
- [26] Mohammad Hossein Ahmadi et al., “Using GMDH Neural Networks to Model the Power and Torque of a Stirling Engine,” *Sustainability*, vol. 7, no. 2, pp. 2243–2255, 2015. [[CrossRef](#)] [[Google Scholar](#)] [[Publisher Link](#)]
- [27] Isa Ebtehaj et al., “GMDH-Type Neural Network Approach for Modeling the Discharge Coefficient of Rectangular Sharp-Crested Side Weirs,” *Engineering Science and Technology, An International Journal*, vol. 18, no. 4, pp. 746-757, 2015. [[CrossRef](#)] [[Google Scholar](#)] [[Publisher Link](#)]
- [28] Tiantian Xie, Hao Yu, and Bogdan Wilamowski, “Comparison between Traditional Neural Networks and Radial Basis Function Networks,” *IEEE International Symposium on Industrial Electronics*, pp. 1194–1199, 2011. [[CrossRef](#)] [[Google Scholar](#)] [[Publisher Link](#)]
- [29] Qiang Xu et al., “Wood Dust Flammability Analysis by Microscale Combustion Calorimetry,” *Polymers (Basel)*, vol. 14, no. 1, p. 45, 2022. [[CrossRef](#)] [[Google Scholar](#)] [[Publisher Link](#)]
- [30] Sarah A. Elawam et al., "Structural Configuration and Thermal Analyses of Composite Films of Poly (methyl methacrylate)/Lead Oxide Nanoparticles," *SSRG International Journal of Applied Physics*, vol. 3, no. 3, pp. 6-14, 2016. [[CrossRef](#)] [[Google Scholar](#)] [[Publisher Link](#)]
- [31] Govmark Datasheet of Micro-Scale Combustion Calorimeter (MCC-2), *Govmark Organ. Inc.*
- [32] Qiang Xu et al., “A PMMA Flammability Analysis Using the MCC: Effect of Specimen Mass,” *Journal of Thermal Analysis and Calorimetry*, vol. 126, no. 3, pp. 1831–1840, 2016. [[CrossRef](#)] [[Google Scholar](#)] [[Publisher Link](#)]
- [33] Umar Ali et al., “A Review of the Properties and Applications of Poly (Methyl Methacrylate) (PMMA),” *Polymer Reviews*, vol. 55, no. 4, pp. 678–705, 2015. [[CrossRef](#)] [[Google Scholar](#)] [[Publisher Link](#)]
- [34] N.Hamid-Zadeh et al., “A Polynomial Model for Concrete Compressive Strength Prediction using GMDH-type Neural Networks and Genetic Algorithm," *Proceedings of the 5th WSEAS International Conference on System Science and Simulation in Engineering*, pp. 13–18, 2006. [[Google Scholar](#)] [[Publisher Link](#)]
- [35] Godfrey C Onwubolu, “Chapter 1,” *GMDH: Methodology and Implementation in Matlab*, pp. 1–24, 2016. [[Google Scholar](#)] [[Publisher Link](#)]
- [36] Rita Yi Man Li, Simon Fong, and Kyle Weng Sang Chong, “Forecasting the REITs and Stock Indices: Group Method of Data Handling Neural Network Approach,” *Pacific Rim Property Research Journal*, vol. 23, no. 2, pp. 123–160, 2017. [[CrossRef](#)] [[Google Scholar](#)] [[Publisher Link](#)]
- [37] Ahmed Amara Konaté et al., “Generalized Regression and Feed-Forward Back Propagation Neural Networks in Modelling Porosity from Geophysical Well Logs,” *Journal of Petroleum Exploration and Production Technology*, vol. 5, no. 2, pp. 157–166, 2015. [[CrossRef](#)] [[Google Scholar](#)] [[Publisher Link](#)]
- [38] Kevin Gurney, *An Introduction to Neural Networks*, 2005. [[Google Scholar](#)] [[Publisher Link](#)]
- [39] M.T. Hagan, and M.B. Menhaj, “Training Feedforward Networks with the Marquardt Algorithm,” *IEEE Transactions on Neural Networks*, vol. 5, no. 6, pp. 989–993, 1994. [[CrossRef](#)] [[Google Scholar](#)] [[Publisher Link](#)]
- [40] T. Chai and R. R. Draxler, “Root Mean Square Error (RMSE) or Mean Absolute Error (MAE)? -Arguments Against Avoiding RMSE in the Literature,” *Geoscientific Model Development*, vol. 7, no. 3, pp. 1247–1250, 2014. [[CrossRef](#)] [[Google Scholar](#)] [[Publisher Link](#)]

- [41] Qiang Xu et al., “Correlation Analysis of Cone Calorimetry Test Data Assessment of the Procedure with Tests of Different Polymers,” *Journal of Thermal Analysis and Calorimetry*, vol. 110, no. 1, pp. 65–70, 2012. [[CrossRef](#)] [[Google Scholar](#)] [[Publisher Link](#)]
- [42] Mohammad Sepehr et al., “Modeling Dynamic Viscosity of N-Alkanes Using LSSVM Technique,” *Energy Sources, Part A: Recovery, Utilization, and Environmental Effects*, vol. 40, no. 16, pp. 1966–1973, 2018. [[CrossRef](#)] [[Google Scholar](#)] [[Publisher Link](#)]